

## Measurement of the Positronium $1^3S_1$ - $2^3S_1$ Interval by Doppler-Free Two-Photon Spectroscopy

Steven Chu and Allen P. Mills, Jr.

*AT&T Bell Laboratories, Murray Hill, New Jersey 07974*

and

John L. Hall

*Joint Institute for Laboratory Astrophysics, National Bureau of Standards  
and University of Colorado, Boulder, Colorado 80303*

(Received 27 February 1984)

We have measured the  $1^3S_1$ - $2^3S_1$  interval in positronium (Ps) to be  $1\,233\,607\,185 \pm 15$  MHz, in agreement to within 1% of the  $\alpha^3R_\infty$  QED prediction. The quoted 12-ppb uncertainty has equal contributions from the measurement of the Ps resonance relative to a  $\text{Te}_2$  absorption line and the calibration of the  $\text{Te}_2$  line relative to the deuterium  $2S_{1/2}$ - $4P_{3/2}$  Balmer line.

PACS numbers: 36.10.Dr, 12.20.Fv

Positronium (Ps),<sup>1</sup> the  $e^+e^-$  bound state, is one of the most fundamental systems available for precision studies. It provides a unique opportunity for studying a purely leptonic two-body system with virtual annihilation interactions and the QED corrections to that system. Until recently, the best information about the Ps level structure was obtained from radio-frequency measurements of the ground-state hyperfine splitting and the  $2^3S_1$ - $2^3P_2$  "Lamb shift."<sup>1</sup> New developments in positron physics and laser spectroscopy now permit precision optical measurements<sup>2</sup> to be made on the triplet Ps energy levels via Doppler-free two-photon spectroscopy. In this Letter, we report the results of a new measurement of the  $1^3S_1$ - $2^3S_1$  interval with a two orders of magnitude increase in the experimental accuracy. This measurement now provides a test of QED corrections in Ps comparable to the rf measurements.

In our experiment Ps was formed by 10-nsec bursts of 50–100 positrons that strike a clean Al(111) target surface in ultrahigh vacuum as described by Chu and co-workers.<sup>2,3</sup> The target was kept at 300°C to desorb the surface state positrons as free thermal Ps in vacuum. The Ps was excited to the  $2^3S_1$  state by two counterpropagating 486-nm laser pulses. Atoms in the  $n=2$  state were ionized with high probability by the intense laser beams. We detected the positrons from the ionization events and recorded the count rate versus laser frequency as the laser was tuned through the  $1^3S_1$ - $2^3S_1$  resonance. Our measurement of the  $1^3S_1$ - $2^3S_1$  interval results from finding the resonance line center and calibrating the laser frequency in terms of known  $D_\beta$  transitions at 486 nm.

The layout of the optical components is summarized in Ref. 3. A Coherent 699-21 actively stabilized cw ring dye laser pumped by a Coherent 3000-K Kr-ion laser was the optical frequency source. Two-thirds of the cw laser output was amplified by a four-stage, single-pass amplifier system transversely pumped by a Lambda-Physik EMG 102E XeCl excimer laser. The cw power (30–60 mW) was amplified into 20–25-mJ, 10-ns laser pulses at  $50 \text{ sec}^{-1}$  with a frequency linewidth of  $\Delta\nu < 70$  MHz. The frequency reference used was a  $\text{Te}_2$  molecular line observed via Doppler-free saturation spectroscopy. A  $\text{Te}_2$  absorption line was found within 50 MHz of half the Ps  $1^3S_1$ - $2^3S_1$  transition frequency. We used a crystal-controlled acousto-optic modulator to create a cw laser sideband 50 MHz higher than the fundamental frequency so that each absorption line in the  $\text{Te}_2$  spectrum had an absorption at the true value,  $\nu_{\text{Te}_2}$ , at  $\nu_{\text{Te}_2} + 50$  MHz, and at the crossover  $\nu_{\text{Te}_2} + 25$  MHz. We could thus position an apparent absorption line near the center of the Ps resonance and simultaneously have an exact calibration of the laser frequency scan rate. A second measurement of the scan rate was provided by the fringes obtained with a  $\frac{1}{2}$ -m-long semi-confocal vacuum Fabry-Perot interferometer. A scanning Michelson interferometer wave meter<sup>4</sup> was used to calibrate to  $\pm 1$  ppm the free spectral range of the  $\frac{1}{2}$ -m interferometer locked to a transmission fringe of a polarization stabilized He-Ne laser<sup>5</sup> with  $< 1$  MHz/day drift rate. Using the calibrated interferometer, we determined the frequency interval between the  $\text{Te}_2$  line  $\nu_{\text{Te}_2}$  and the deuterium  $n=2 \rightarrow 4$  transitions measured in a

Wood's discharge tube.

The Ps atoms were generated inside a flat-flat interferometer<sup>3</sup> mounted in the ultrahigh vacuum chamber ( $P = 2 \times 10^{-10}$  Torr). The interferometer (free spectral range = 450 MHz, finesse  $\approx 35$ ) served the dual purpose of forming the counterpropagating light beams needed for two-photon Doppler-free spectroscopy and acting as a final frequency filter for the laser source. The interferometer was continuously adjusted for maximum pulsed laser transmission. Each 10-nsec-wide laser pulse was stretched into a nearly Fourier-transform limited 40-nsec pulse. The short-term  $\pm 1.5 \times 10^{-4}$  rad pointing instability of the dye amplifier increased the time-averaged laser bandwidth to 30–35 MHz. The average pointing error was adjusted to be less than  $\pm 3 \times 10^{-5}$  rad rms. The residual pointing error averaged over ten scans,  $\Delta\phi = \pm 10^{-5}$  rad, leads to a first-order Doppler shift error in our measurement of  $2(\nu/c) \cdot \Delta\phi = \pm 3 \times 10^{-9}$ . A low electric field (3 V/cm) in the Ps ionization region extracted the  $e^+$  ionization fragments while minimizing the dc Stark shift of the atom. A grid was used to accelerate the positrons to a final energy of 200 eV and thence to a microchannel plate single-particle detector as described in Ref. 2.

Figure 1 shows a single 5-min scan of the Ps resonance along with the simultaneously recorded  $\text{Te}_2$  resonance line and the frequency marker. The major systematic effects in the measurement of the Ps resonance relative to the  $\text{Te}_2$  line are (i) the fre-

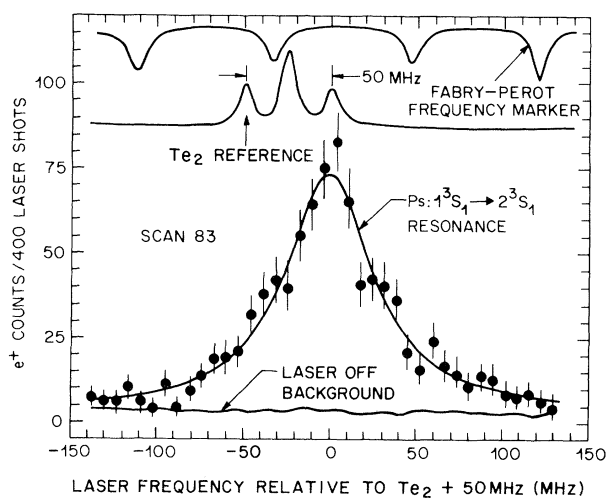


FIG. 1. Resonant three-photon ionization of positronium due to  $1^3S_1 + 3h\nu \rightarrow 2^3S_1 + h\nu \rightarrow e^+ + e^-$ . For this scan, the line center was  $25.9 \pm 2.7$  MHz above the  $\text{Te}_2$  line, with  $\chi^2/\nu = 29.97/36$ .

quency offset between the cw dye laser and the pulsed beam resonant in the ultrahigh vacuum Fabry-Perot cavity, (ii) the second-order Doppler shift (time dilation) due to the Ps motion relative to the laser frame of reference, and (iii) the ac Stark shift introduced by the intense laser beam. We measured the frequency offset between the cw dye laser and the pulsed laser beam transmitted through the vacuum Fabry-Perot sample region using a scanning confocal Fabry-Perot interferometer having a 300-MHz free spectral range and a resolution of about 2 MHz. The offset was measured three or four times while the laser was tuned to the Ps resonance for each run. The transmitted pulsed laser frequency was typically 20 MHz lower than the cw frequency.

We obtained two sets of runs which can be used to deduce the  $1^3S_1$ - $2^3S_1$  interval in Ps. Each scan of the photoionized  $e^+$  count rate versus laser frequency was fitted to a Lorentzian to obtain the line center relative to the  $\text{Te}_2$  reference line, the peak count rate, and the linewidth. The measured laser-off count rate was used as a baseline for the Lorentzian. We obtained several runs at a constant power  $P$  with various time delays  $t$  between the arrival of the  $e^+$  pulse at the target and the center of the laser pulse in the vacuum Fabry-Perot cavity. Figure 2 shows the line centers for one run obtained at a measured average power  $P = 43$  mW transmitted through the vacuum Fabry-Perot. The center of the  $\sim 6$ -mm-diameter laser beam was measured to be  $z = (3.8 \pm 0.5)$  mm from the Al target surface. The longitudinal Ps velocity is  $v_z = z/t$  and the horizontal axis in Fig. 2 is  $(v_z/c)^2$ . Figure 3 shows the line centers, linewidths, and amplitudes

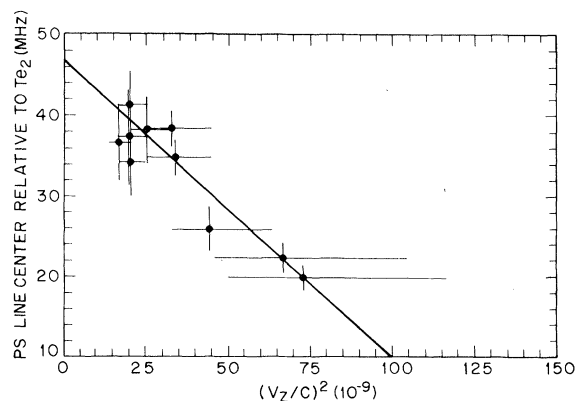


FIG. 2. Ps line center relative to the  $\text{Te}_2$  reference line plotted vs  $v_z^2/c^2$  showing the second-order Doppler shift. The straight line intercepts the  $v_z^2 = 0$  axis at  $46.7 \pm 3.3$  MHz with  $\chi^2/\nu = 8.13/8$ .

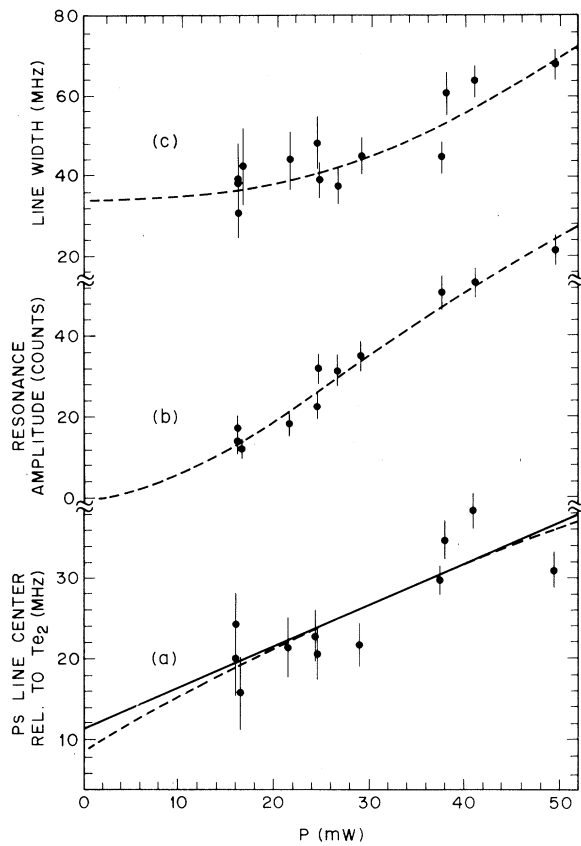


FIG. 3. Frequency shift, linewidth, and resonance amplitude plotted vs transmitted laser power. The simultaneous fit of three theoretical curves to the data is given by the dashed lines. The simple quadratic Stark shift is shown by the solid line and is listed in Table I.

for the same run obtained with a constant  $(v_z/c)^2 = 33 \times 10^{-9}$  and various transmitted powers. The uncertainty in  $(v_z/c)^2$  displayed in Fig. 2 arises from our inability to determine an exact effective delay time because of the combined effects of the temporal laser pulse shape, the time dependence of the two-photon plus ionization transition, and the transit of the Ps through the laser beam.

The reduction of our measurements to an absolute value for  $\nu_{Ps}(1^3S_1-2^3S_1)$  is summarized in Table I. The first entries in Table I are the Ps line center measurements relative to the  $Te_2$  line for the two runs. These values have been corrected for the laser frequency offset and extrapolated to zero red shift using a least-squares fit of a straight line to the red-shift data (see Fig. 2). The second entries in Table I are the ac Stark shift corrections obtained from a linear least-squares fit to the line center versus laser power measurements [cf. solid line in Fig. 3(a)]. Saturation and time dependence effects will cause deviations from a linear fit which we have taken into account by an appropriate increase in the linear least-squares error estimate. The dashed lines in Fig. 3 indicate our present best theoretical treatment of these effects, showing the resonance amplitude [Fig. 3(b)] and the linewidth [Fig. 3(c)] as a function of laser power. The  $\approx 34$ -MHz linewidth at zero laser intensity is attributed to the laser beam pointing instabilities relative to the vacuum Fabry-Perot cavity. Table I also shows the results of three measurements of the difference between the  $Te_2$  line and the deuterium  $2S_{1/2}-4P_{3/2}$

TABLE I. Measurements and calculations used to obtain the Ps  $1^3S_1-2^3S_1$  interval. Frequencies in megahertz.

$\frac{1}{2} \nu_{Ps} - \nu_{Te_2} (v_z^2/c^2 \rightarrow 0)$	$+ 45.1 \pm 4.2$	$+ 46.7 \pm 3.3$
ac Stark shift	$- 15.2 \pm 7.3$	$- 21.6 \pm 5.0$
$\frac{1}{2} \nu_{Ps} - \nu_{Te_2} (v_z^2/c^2 \rightarrow 0, P \rightarrow 0)$		$+ 26.7 \pm 4.9$
$\nu_{Te_2} - \nu_D$		$+ 114\,410.4 \pm 1.8$
dc Stark shift		$+ 17.0 \pm 5.0$
$\nu_D - \frac{3}{16} R_\infty c$ (theory)		$- 156\,266.041$
$\frac{1}{2} \nu_{Ps} - \frac{3}{16} R_\infty c$		$- 41\,771.9 \pm 4.9 \pm 5.3$
Motional Stark and Zeeman		$- 1.14$
dc Stark shift		$- 0.07$
First-order Doppler shift		$0.0 \pm 1.9$
$\nu_{Ps}(1^3S_1-2^3S_1)_{exp}$		$\frac{3}{8} R_\infty c - 83\,546.3 \pm 10.5 \pm 10.6$
$\nu_{Ps}(1^3S_1-2^3S_1)_{th}$		$\frac{3}{8} R_\infty c - 83\,533.06(2) \pm (10)$

Balmer line. The frequency of the  $D_\beta$  line relative to  $\frac{3}{16}R_\infty c$  is obtained from the calculations of Erickson.<sup>6</sup> The major systematic uncertainty is the Stark shift of the  $D_\beta$  line due to the dc electric field in the discharge tube. The average electric field is measured to be  $6 \pm 1$  V/cm, but the appearance of fixed striations along the length of the tube suggest a nonuniform electric field.<sup>7</sup> We estimate the correction<sup>8</sup> and uncertainty to be  $17 \pm 5$  MHz. The next entries in Table I are the following systematic corrections: (i) the motional<sup>9</sup> Stark and Zeeman shifts calculated for 0.017-eV Ps in a 150-G field, (ii) the dc Stark shift calculated for Ps in a 3 V/cm field, and (iii) the residual first-order Doppler shift. The final entries are the resulting value of the Ps  $1^3S_1$ - $2^3S_1$  interval relative to  $\frac{3}{8}R_\infty c$  (the nonrelativistic Schrödinger value) and the theoretical prediction of Fulton.<sup>10</sup> He calculates the  $\alpha^3 R_\infty$  correction to be  $-1527$  MHz, and our result verifies this with less than 1% uncertainty. Theory and experiment differ by  $(13 \pm 10.5 \pm 10.6)$  MHz where the first error is from the Ps measurement relative to the  $Te_2$  line and the second error is from the absolute  $Te_2$  calibration. In comparing theory and experiment we note that most of the  $\alpha^4 R_\infty$  terms have not been calculated and might be expected to be of order 10–20 MHz.

Using the present value of the Rydberg<sup>11</sup> accurate to one part in  $10^9$  we obtain for the full Ps  $1^3S_1$ - $2^3S_1$  interval  $1\,233\,607\,185 \pm 15$  MHz. As a corollary, note that we have implicitly assumed that the Ps Rydberg ( $R_{Ps}$ ) is exactly  $\frac{1}{2}R_\infty$ . The present agreement between theory and experiment implies that  $|m_{e^+} - m_{e^-}| < 4 \times 10^{-8} m_{e^-}$  at a 90% confidence level, a slight improvement over the result obtained from the  $e^+$ ,  $e^-$  trap experiments of Schwinberg, Van Dyck, and Dehmelt.<sup>12</sup> Given the current progress in laser spectroscopy, it should be possible in the near future to measure this energy interval to a precision significantly better than the 1-MHz natural linewidth leading to even better measurements of  $R_{Ps}$  and of QED effects on the

two-body system.

We gratefully acknowledge the assistance of W. Busis, discussions with G. Holtom, K. Lynn, P. Mohr, P. Pappas, J. Sapirstein, and valuable support from Coherent, Inc., The Regional Laser Facility of the University of Pennsylvania, Spectra Physics, The Regional Laser Facility at Massachusetts Institute of Technology, and R. L. Barger of Lase-angle Co. The work done at the Joint Institute for Laboratory Astrophysics is supported by the National Bureau of Standards, the National Science Foundation, and The Office of Naval Research.

<sup>1</sup>See A. Rich, *Rev. Mod. Phys.* **53**, 127 (1981), and references therein.

<sup>2</sup>S. Chu and A. P. Mills, Jr., *Phys. Rev. Lett.* **48**, 1333 (1982); A. P. Mills, Jr., and S. Chu, in *Atomic Physics 8*, edited by A. Rosen and S. Svanberg (Plenum, New York, 1982), p. 83.

<sup>3</sup>S. Chu, A. P. Mills, Jr., and J. L. Hall, in *Laser Spectroscopy VI*, edited by H. P. Weber and W. Lüthy (Springer-Verlag, Heidelberg, 1983), p. 28.

<sup>4</sup>S. A. Lee and J. L. Hall, in *Laser Spectroscopy III*, edited by J. L. Hall and J. L. Carlsten (Springer-Verlag, Heidelberg, 1977), p. 421.

<sup>5</sup>R. Balhorn, H. Kunzman, and F. Lebowsky, *Appl. Optics* **11**, 742 (1972).

<sup>6</sup>G. W. Erickson, *J. Phys. Chem. Ref. Data* **6**, 831 (1977). The value of  $\nu_D$  has been updated using the latest value of  $R_\infty$  from Ref. 11.

<sup>7</sup>L. B. Loeb, *Fundamental Processes of Electronic Discharge in Gases* (Wiley, New York, 1939).

<sup>8</sup>V. Rojansky, *Phys. Rev.* **33**, 1 (1929).

<sup>9</sup>M. L. Lewis and V. W. Hughes, *Phys. Rev. A* **8**, 625 (1973).

<sup>10</sup>T. Fulton, *Phys. Rev. A* **26**, 1794 (1982).

<sup>11</sup>S. R. Amin, C. D. Caldwell, and W. Lichten, *Phys. Rev. Lett.* **47**, 1234 (1981).

<sup>12</sup>P. B. Schwinberg, R. S. Van Dyck, Jr., and H. G. Dehmelt, *Phys. Lett.* **81A**, 119 (1981). The much more precise measurements of  $(g_+ - 2)/(g_- - 2)$  by the same authors in *Phys. Rev. Lett.* **47**, 1679 (1981) tells us little about  $m_+/m_-$ .